NASA TECHNICAL NOTE

NASA TN D-4416

NASA TN D-4416

EXPERIMENTAL INVESTIGATION OF REACTION CONTROL, STORABLE BIPROPELLANT THRUSTORS

by R. James Rollbuhler

Lewis Research Center

Cleveland, Ohio

NATIONAL AERONAUTICS AND SPACE ADMINISTRATION • WASHINGTON, D. C. • APRIL 1968

EXPERIMENTAL INVESTIGATION OF REACTION CONTROL, STORABLE BIPROPELLANT THRUSTORS

By R. James Rollbuhler

Lewis Research Center
Cleveland, Ohio

NATIONAL AERONAUTICS AND SPACE ADMINISTRATION

For sale by the Clearinghouse for Federal Scientific and Technical Information
Springfield, Virginia 22151 – CFSTI price $3.00

EXPERIMENTAL INVESTIGATION OF REACTION CONTROL, STORABLE BIPROPELLANT THRUSTORS

by R. James Rollbuhler

Lewis Research Center

SUMMARY

In order to evaluate the performance of low-thrust, chemical bipropellant rocket thrustors for possible applications in spacecraft reaction control systems, an experimental investigation was conducted with readily available thrustors. The thrustors were designed for a thrust of less than 5 pounds force (22.2 N), combustion-chamber pressures of 100 pounds per square inch absolute (68.9 N/cm^2) or less, and for use with nitrogen tetroxide - hydrazine-type propellants. A highly instrumented altitude test facility was used to test each of the thrustors over a range of test durations and oxidizer to fuel ratios.

The maximum specific impulse obtained was 262 pounds force per pound mass per second (2570 (N)(sec)/kg), and the maximum characteristic velocity was 5200 feet per second (1588 m/sec). Total impulses were measured for run times as short as 10 milliseconds. The average value of the specific impulse, at minimum run times, was about 25 percent of the maximum specific impulse for the same thrustor. Also reported are response times and combustor-wall temperatures.

INTRODUCTION

Recent space missions have indicated the increasing need for spacecraft with the ability to control closely their attitude and orbit position or trajectory. These requirements have been met in most cases by mass expulsion thrustors, such as chemical rockets and cold-gas thrustors. For both attitude and orbit control, there have been increasing requirements for the delivery of small impulse bits to control the spacecraft attitude more closely or to make minor orbit or trajectory corrections. Small impulse bits imply either short firing times or low values of thrust. The reduction of firing time is practically limited by the reaction time of propellant valves and the deteriorating performance of the thrustor because of poor reaction kinetics and high thermodynamic losses. Therefore, low values of impulse bit have been obtained principally by the use of smaller thrustors.

One form of small thrustor that has found extensive applications is one employing cold gas such as nitrogen as a mass expellant. Although the advantages of this thrustor system lie in its simplicity, the specific impulse of the propellant is very low compared with the conventional propellant combinations. Thus, for systems with long mission times requiring a substantial total impulse, the propellant weight often becomes prohibitively large. Therefore, interest has increased in small thrustors that employ the conventional propellant combinations to produce a high specific impulse.

Presented herein are the results of experiments conducted to study the performance of several thrustors that use nitrogen tetroxide and a mixture of 50 percent unsymmetrical dimethylhydrazine (UDMH) and 50 percent hydrazine as propellants and range in thrust from 1/2 to 5 pounds (2.22 to 22.2 N). The two aspects of engine performance of prime interest were the efficiency of the thrustor during normal steady-state operation and the pulsing performance of the thrustors in terms of impulse bit as a function of firing time. Certain other engine performance characteristics that were noted during the study included the relation of thrust to combustion-chamber pressure, combustion time lags, temperature histories, and thrust buildup patterns during pulsing operation.

SYMBOLS

A_t thrustor nozzle throat cross-sectional area, $in.^2$; cm^2

C^* characteristic exhaust velocity, ft/sec; m/sec

C_f thrust coefficient

F thrust, lb force; N

g_c gravitational acceleration, 32.2 ft/sec^2; 9.81 m/sec^2

I_{sp} specific impulse, (lb force)(sec)/lb mass; (N)(sec)/kg

I_t total impulse, (lb force)(sec); (N)(sec)

L^* characteristic thrustor length, in.; cm

O/F oxidizer-fuel mass-flow ratio

P_c combustion chamber pressure, psia; N/cm^2

W_t total propellant weight flow rate, lb mass/sec; kg/sec

APPARATUS AND PROCEDURE

Test Hardware

Seven different thrustor assemblies, complete with propellant control valves, and four alternate valve assemblies were obtained for this program. All were essentially off-the-shelf designs. Because the only criteria specified were the maximum thrust and the type of propellants, the assemblies came in a variety of sizes, weights, dimensions, and materials. Some had altitude expansion nozzles while others had sea-level expansion nozzles. The rated combustion-chamber pressure varied from 35 to 100 pounds per square inch absolute (24.1 to 68.9 N/cm^2). The construction materials were another variable to consider for each of the thrustors.

The testing of two of the four alternate valve assemblies was discontinued because they proved to be incompatible with the propellants being used.

Thrustor assemblies. - Each assembly consisted of a combustion chamber and an expansion nozzle, a propellant injector, and valve assemblies for on-off control of the propellant flows. The seven thrustor assemblies and two of the alternate valve assemblies are pictured in figure 1, and their pertinent physical data are listed in table I.

The thrustors and the individual valves are identified numerically. Thrustor 7 initially had valves that proved unsuitable; therefore, the assembly was modified so that either valve unit 8 or 9 could be integrated into the assembly. Valve unit 8 is shown mounted on thrustor 7, and valve unit 9 is shown both assembled and disassembled in figure 1.

Injection techniques. - Several different injection patterns were used to flow the propellants into the thrustor combustion chambers. Thrustor 1 injected an oxidant and fuel jet, each 180° apart, on a wedge so that the resulting sprays impinged on each other. Thrustor 2 used three pairs of impinging jets with each pair being a fuel impinging on an oxidizer jet. Thrustors 3 and 6 each used a single pair of impinging jets. Thrustors 4 and 5 had two fuel jets impinging on an axial oxidizer jet. Thrustor 7 utilized a spray jet for the fuel and a similar spray jet for the oxidizer. The sprays, 180° apart, entered the chamber through the side wall and were directed toward the head of the chamber rather than toward the combustor throat.

Combustion chambers and expansion nozzles. - Thrustors 1 to 6a were designed to operate over extended continuous durations (i.e., longer than 10 sec). Thrustors 3 to 5 had refractory metal combustion chambers and nozzles that were coated with various surface coatings to prevent high-temperature-metal oxidation. Thrustor 4 had a stainless-steel chamber and nozzle; for extended run durations, the interior of thrustor 4 was flame sprayed with aluminum oxide. For runs of only a few seconds, heat-sink, rather than radiation, cooling was satisfactory.

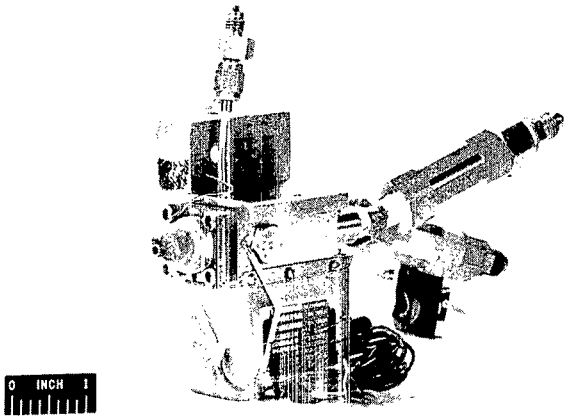

C-74756

(a) Thrustor 1.

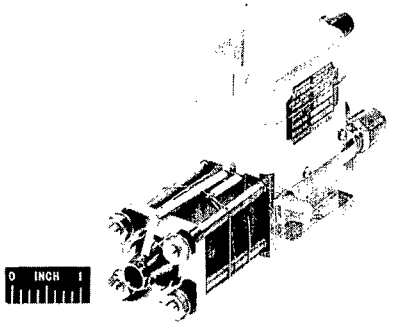

C-71929

(b) Thrustor 2.

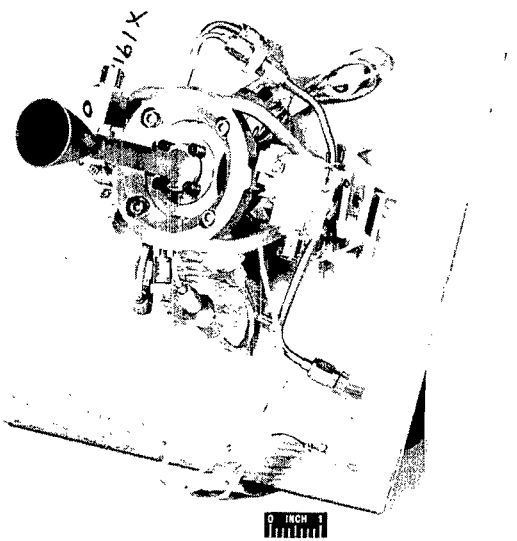

C-71462

(c) Thrustor 3.

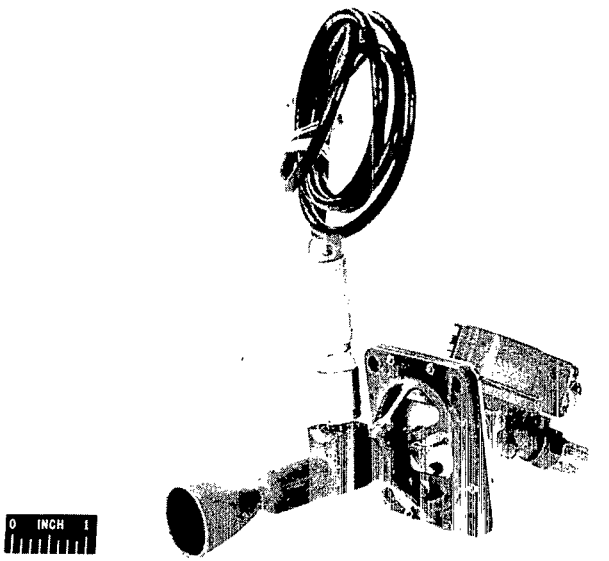

C-74754

(d) Thrustor 4.

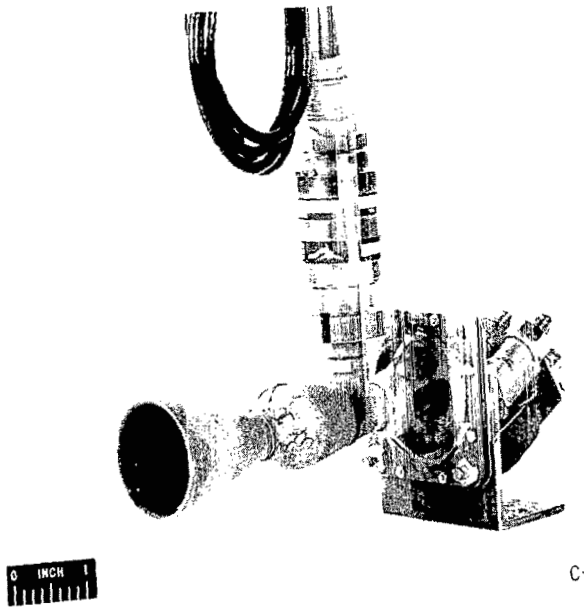

C-74750

(e) Thrustor 5.

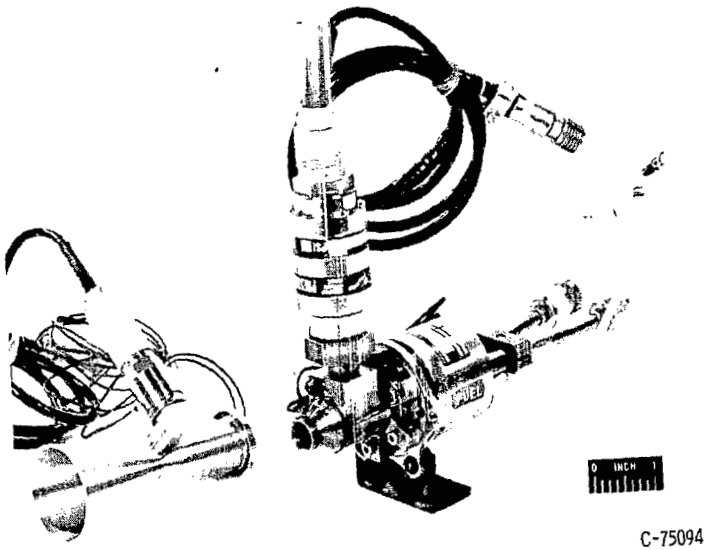

C-75094

(f) Thrustors 6b and 6c.

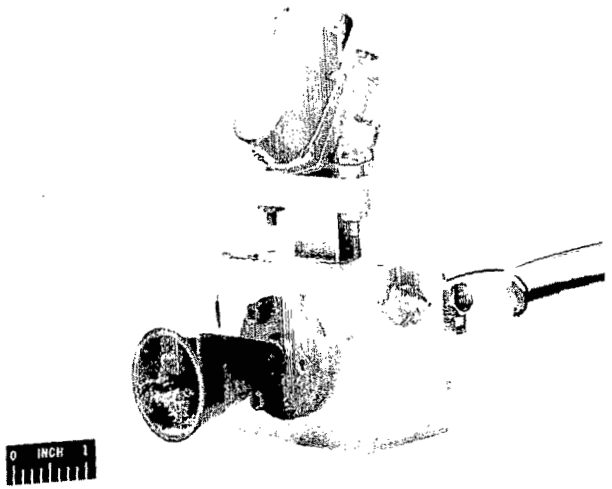

C-74752

(g) Valve 8 on thrustor 7.

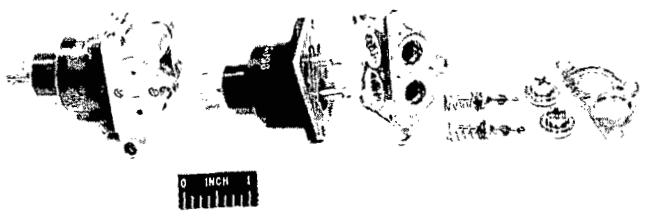

C-65863

(h) Valve 9.

Figure 1. - Bipropellant thrustor and valve assemblies.

TABLE I. - PHYSICAL CHARACTERISTICS OF LOW THRUST, LIQUID BIPROPELLANT ROCKET THRUSTOR

Thrustor	Rated combustion-chamber pressure		Rated thrust		Combustor throat diameter		Nozzle expansion ratio	Thrustor characteristic length		Combustion-chamber volume		Combustion-chamber wall material	Nozzle material	Protective wall coating	Number of propellant injector parts		Propellant control valve type	Valve operating current at dc of 28 V, A
	psia	N/cm^2	lb force	N	in.	mm		in.	cm	$in.^3$	cm^3				Fuel	Oxidizer		
1	75	51.6	0.5	22.2	0.082	2.08	1.6	20	50.8	0.105	1.72	Tungsten	Tungsten	None	1	1	Torque motor	0.3
2	75	51.6	5.0	22.2	.287	7.29	1.46	20	50.8	1.25	20.5	Graphite	Tungsten	None	3	3	Torque motor	.4
3a	96	56.2	5.0	22.2	.193	4.91	40	6	15.2	.12	1.97	TZM molybdenum alloy	TZM molybdenum alloy	Molybdenum disilicide	1	1	Solenoid	.6
3b	96	56.2	5.0	22.2	.193	4.91	40	11	27.9	.37	6.07	TZM molybdenum alloy	TZM molybdenum alloy	Molybdenum disilicide	1	1	Solenoid	.6
4	50	34.4	1.0	4.45	.115	2.92	60	38	96.5	.303	4.97	Tantalum-tungsten alloy	Tantalum-tungsten alloy	Silicide diffusion	2		Torque motor	.3
5	60	41.4	5.0	22.2	.242	6.15	40	23	58.5	1.08	17.7	Tantalum-tungsten alloy	Tantalum-tungsten alloy	Silicide diffusion	2		Torque motor	.5
6a	35	24.1			.321	8.16	40	8	20.3	.647	10.6	TZM molybdenum alloy	TZM molybdenum alloy	Molybdenum disilicide	1		Solenoid	.3
6b	35	24.1			.351	8.92	20	8	20.3	.78	12.8	304 Stainless steel	304 Stainless steel	Aluminum oxide			Solenoid	.3
6c	35	24.1			.367	9.33	1.6	8	20.3	.85	13.9	304 Stainless steel	304 Stainless steel	Aluminum oxide			Solenoid	.3
7	100	68.9	"	"	.176	4.47	62	60	152	1.58	25.9	304 Stainless steel	Tantalum-tungsten alloy	Aluminide	"	"	Torque motor	0.2 to 0.3

Propellant valves. - The propellant control valves were fast-acting, 28-volt, torque motor or solenoid-actuated types. The solenoid type employs a 28-volt direct-current magnetic armature to retract a spring-loaded poppet from the propellant-sealing orifice. The torque valve employs a single electromagnetic actuation mechanism operating a mechanical linkage that controls the opening and closing of the different propellant orifices. The actuation mechanism is exterior to the flow stream, and the linkage enters the stream through a flexure sleeve or joint. In most cases, the valves could be removed from their respective thrustors for servicing.

The valve operating power was supplied from a 28-volt direct-current source. The current consumed by each valve is given in table I. The value given is for a nominal current while the valve was in a steady-state operating condition; initial valve opening conditions resulted in a much higher (50 to 100 percent) current value.

Test Facilities

The thrustors and their associated propellant control valves were tested in a test facility that handles the propellants nitrogen tetroxide and a mixture of 50 percent hydrazine and 50 percent unsymmetrical dimethylhydrazine (UDMH). The thrustors were fired in a vacuum environment of 10 millimeters of mercury (1333 N/m^2) or less. They were mounted on the thrust stand inside a 1500-cubic foot (42.5-cu. m.) vacuum tank (see fig. 2). Mechanical vacuum pumping was capable of maintaining fully expanded nozzle gas flow of all the thrustors.

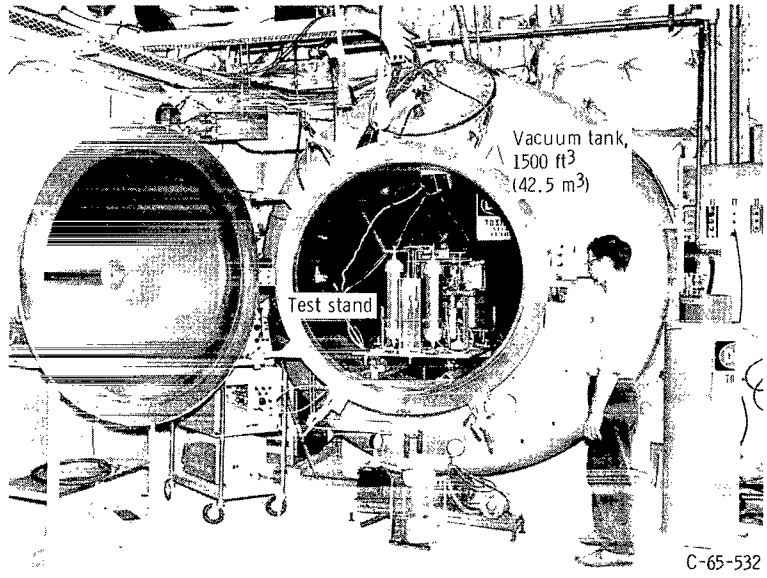

Figure 2. - Vacuum test facility.

The thrust stand was especially designed for testing thrustors that have a thrust level of less than 10 pounds (44.5 N). The thrustor was mounted horizontally on top of the stand (see fig. 3). The stand is a compound pendulum that uses a closed-loop elec-

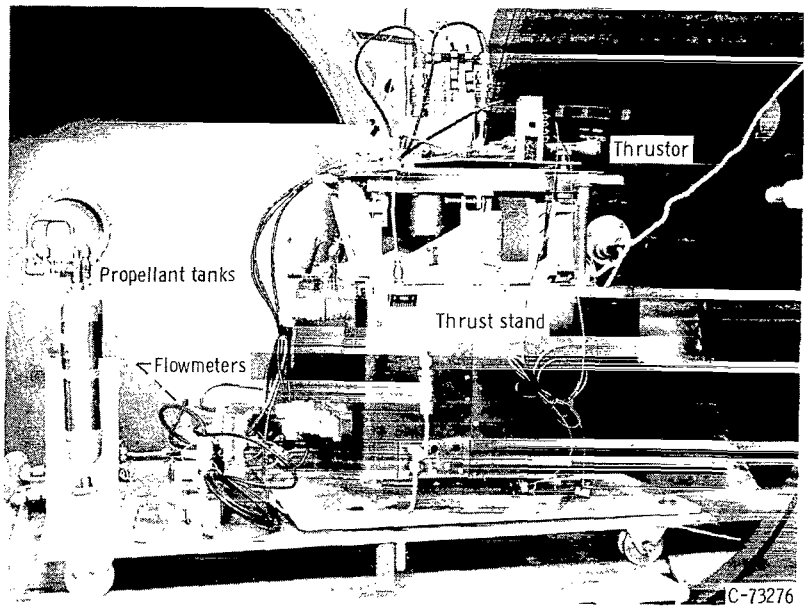

Figure 3. - Thrust stand in 1500-cubic-foot (42.5-cu-m) vacuum tank.

tronic force generating network in a null-balance system for indicating thrust and total impulse. A more complete description of this stand is given in the appendix. Physical calibration of the stand indicated that the thrust data error was ±1.5 percent up to a frequency of 88 cps (88 Hz).

The fuel and oxidizer liquid propellant systems were directly behind the thrust stand (see fig. 3). Each propellant system consisted of a supply tank connected to the thrustor control valve by means of tubing that contained propellant flowmeters. The flow rate of the propellant was controlled by the supply tank pressure.

Instrumentation

In each propellant system, as many as three different flowmeters were placed in series to verify flow rate measurements. These types of flowmeters were orifice differential pressure, turbine, and remote-reading rotameter. The calibration of these flowmeters with actual propellants is described in the appendix. The orifice flowmeter gave the most dependable data over a range of operating conditions. Its steady-state accuracy was ±2 percent of the true flow rate, and its transient response was 0 to 90 percent of the maximum flow within 500 milliseconds.

Besides thrust and flow-rate data, propellant pressures and temperatures,

combustion-chamber pressure, and combustor-wall temperatures were also measured. The pressures were measured with strain-gage pressure transducers, which were calibrated against a precision gage so that the test data accuracy was ±1 percent. The frequency response of the combustion-chamber pressure instrumentation was in the range of 150 to 175 hertz. The method of determining this range is presented in the appendix. The temperatures were measured with thermocouples, and the reading precision of their data signals was $\pm 1^{\circ}$ for the propellants and $\pm 5^{\circ}$ for the combustor-wall temperatures.

All the data signals were recorded on a high-speed (1 to 80 in. or 2.5 to 200 cm of record per sec) oscillograph recorder located in the facility control room (shown in fig. 4). The frequency response of the oscillograph galvanometers varied from 30 to 3000 hertz, depending on the requirements of the variable being recorded. Various problems in verifying test temperatures are mentioned in the appendix.

Test Operations

The thrustor to be tested was rigidly mounted horizontally on top of the thrust stand. The propellant system was connected to the thrustor, and the systems were then pressure checked. The data sensors were calibrated, and the control system was checked out. After the propellant tanks had been filled, the vacuum tank was sealed and the tank pressure was reduced to less than 10 millimeters of mercury (1333 N/m^2).

Test operations were controlled and recorded in a control room remote from the vacuum tank (see fig. 4). For each test, the sequence of events was controlled automatically. When the run button was pushed, the instrumentation recorder began, and then the thrustor propellant control valves were energized. The propellant flow rate to the thrustor was regulated by varying the pressure in the propellant supply tanks. The thrustor firing time could be varied between 10 milliseconds and 600 seconds as could the time between firings. After a preset single or multiple firing, the recorder automatically shut down while the propellant lines and thrustor were purged.

For the testing of a given thrustor, the pressure in the propellant run tanks was varied from test to test to find the optimum thrust at different oxidizer-fuel ratios. Although the individual fuel and oxidizer flow rates were varied, their combined flow rate was kept near a constant value. Once the optimum oxidizer-fuel ratio was determined, it was retained while the thrustor on and off times were varied.

Of all the thrustors tested, only thrustor 1 failed to deliver repeatable performance. This thrustor was tested at both sea-level and vacuum-environment conditions, but the data were erratic and fluctuated over a wide amplitude. The problem was apparently the propellant injection technique; in spite of the 10-micron (10^{-7}-m) propellant inlet filters, the injection ports slowly plugged during each test. The propellant flows decreased erratically as the injection pressure increased to that of the driving pressure in the supply tanks. Each port, which was less than 0.01 inch (0.00254 m) in diameter, had to be

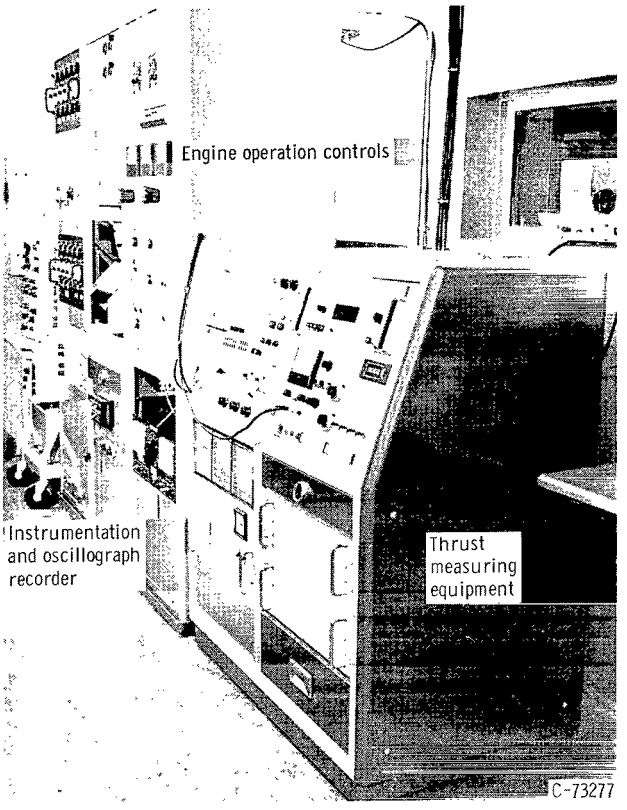

Figure 4. - Control room of vacuum facility.

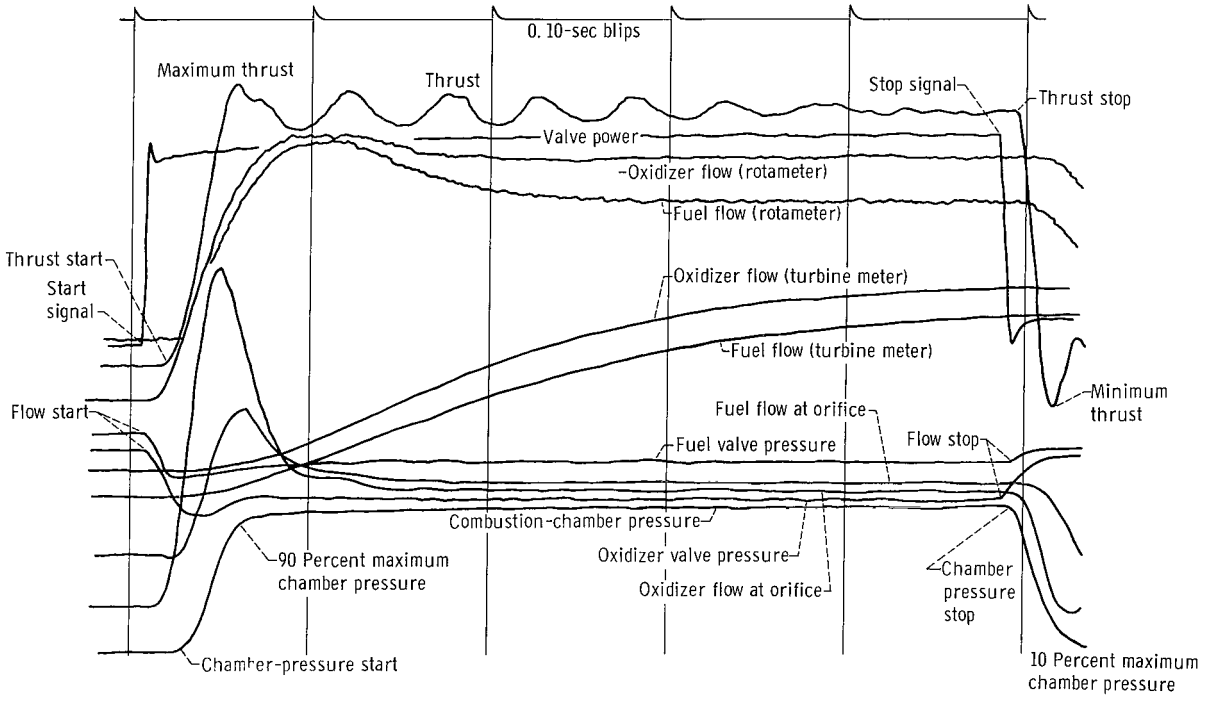

Figure 5. - Typical 500-millisecond test record.

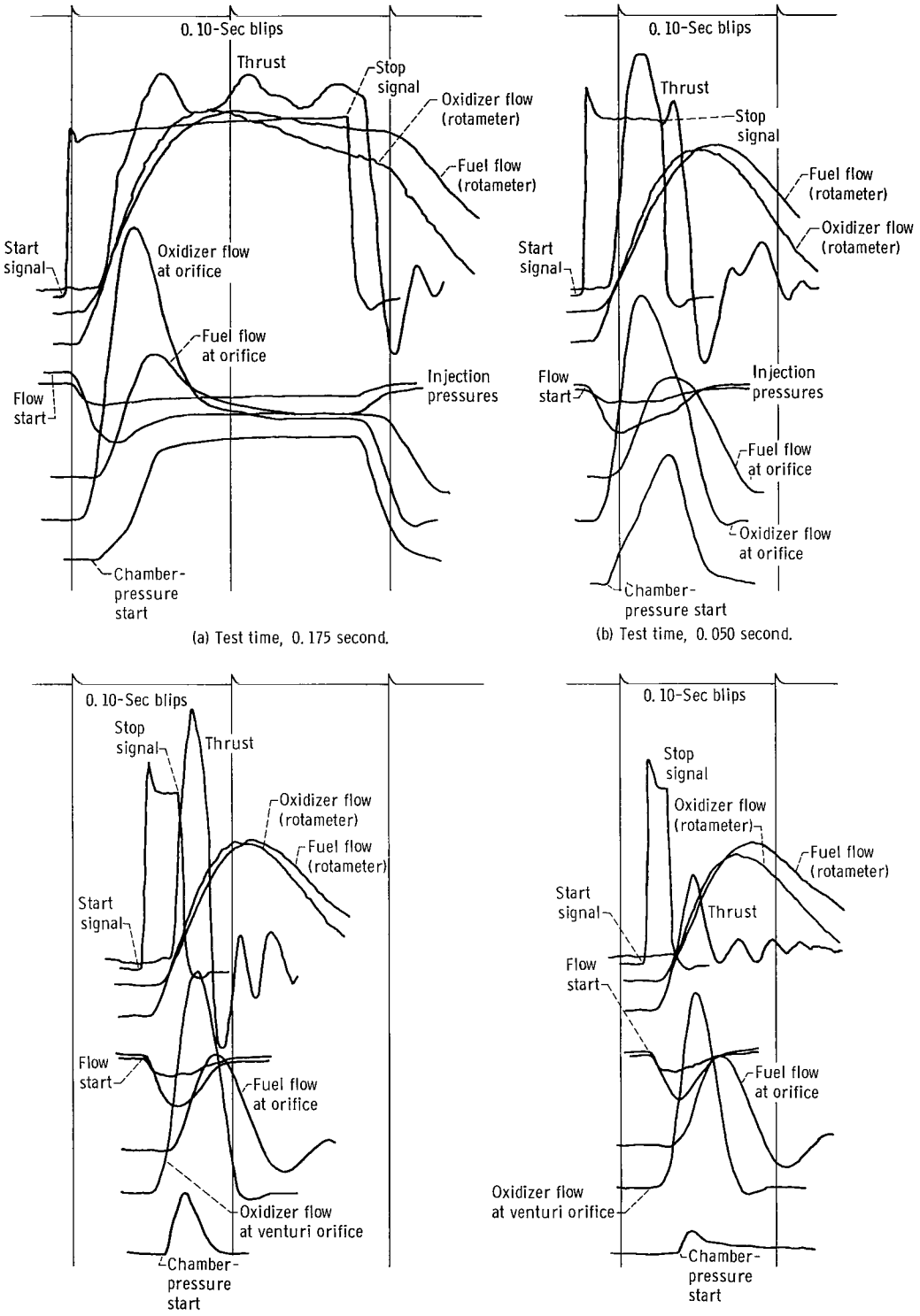

Figure 6. - Disappearance of equilibrium conditions as test durations decreased.

reamed clean to restore the original injection pressure drop. Because of this operating problem, equilibrium and repeatable performance data could not be obtained to include in this report.

Data Analysis

All the test data were recorded on an oscillograph recorder. A typical 500-millisecond-run record is shown in figure 5. The data signals from the transducers (and thermocouples not shown in fig. 5) are expressed as a voltage change representing a known data value. The run duration is defined as the time from the start of valve power to the time the power is stopped.

Equilibrium data conditions for all the thrustors were attained after 500 milliseconds of steady-state thrustor operation. At this equilibrium point, the test data were used to calculate the steady-state performance. However, as test durations were made shorter (fig. 6), equilibrium conditions were no longer apparent. The propellant flow consisted of a surge, the thrust tended toward a shock wave, and pressures had only begun to increase when the test ended. Because of these conditions, the instantaneous data values for the short-duration tests were not reliable.

To obtain performance data from the short-duration runs (fig. 6), the thrust and flow rate signals were integrated over the duration of each test. The tests were repeated at the same operating conditions until repeatable performance data were obtained. From such integrated data, average instantaneous data values could be obtained. Thus, the performance data from tests of 500 milliseconds or longer are based on actual instantaneous conditions; data from shorter duration runs are based on average conditions over the time span of the test.

DISCUSSION OF RESULTS

Steady-State Performance

The experimental results of the investigation of several typical low-thrust, bipropellant, chemical thrustor assemblies are presented in table II.

Thrustor combustion efficiency. - The combustion efficiency of each thrustor was determined as a function of the oxidizer-fuel ratio in terms of characteristic velocity C^*, which is defined as the product of the combustion chamber pressure P_c the thrustor throat cross-sectional area A_t, and the gravitational acceleration constant g_c, all divided by the total propellant weight flow rate W_t

$$C^* = \frac{(g_c)(P_c)(A_t)}{W_t}$$

The combustion efficiency is the ratio of the experimentally determined C^* to the theoretical C^*. The theoretical data are based on an assumption of frozen equilibrium expansion of the combustion gases; that is, after the propellants react in the combustor, the products do not change in flowing through the thrustor throat and expansion nozzle (unpublished data obtained by S. Gordon and E. Norris of Lewis).

TABLE II. - RESULTS OF INVESTIGATION OF LOW-THRUST BIPROPELLANT CHEMICAL THRUSTOR ASSEMBLIES

Quantity	Thrustor					
	2	3	4	5	6	7
Maximum characteristic velocity, ft/sec; m/sec	4700; 143	5190; 158	5000; 153	4620; 141	4400; 134	4960; 151
at oxidant-fuel ratio of	1.5	1.4	0.8	1.4	1.6	2.1
for theoretical frozen characteristic velocity, ft/sec; m/sec	5500; 168	5580; 170	5380; 164	5550; 169	5500; 168	5430; 166
Maximum specific impulse, (lb force)(sec)/lb mass; (N)(sec)/kg	196; 1920	261; 2560	262; 2570	238; 2340	205; 2010	260; 2550
at oxidant-fuel ratio of	1.3	1.4	1.1	1.4	1.6	2.0
for theoretical frozen specific impulse, (lb force)(sec)/lb mass; (N)(sec)/kg	240; 2360	315; 3090	313; 3070	313; 3070	308; 3020	315; 3090
Specific impulse after 100 m sec of run time, (lb force)(sec)/lb mass; (N)(sec)/kg	138; 1352	180; 1768	181; 1777	195; 1913	145; 1422	126; 1238
Thrustor valve response delay, m sec	11	14	10	4	10	6
Thrustor ignition delay, m sec	14	4	43	27	6	299
Thrustor startup delay to 90 percent of maximum thrust, m sec	35	30	109	50	26	704
Maximum thrustor wall temperature recorded, ^{o}F; ^{o}K	1544; 1113	2371; 1572	2107; 1425	1792; 1250	756; 676	1031; 830

In figure 7 the C^* performance data for each of the tested thrustors are presented as a function of the ratio of the oxidizer-fuel weight flow rate. The C^* data are shown as an average curve with the data scatter being ±4 percent or less on either side of the curve in terms of performance, and ±4 percent in terms of the oxidant fuel ratio O/F. For clarity, the average performance curves are shown separately for each thrustor along with the theoretical frozen C^* curves for each thrustor (theoretical data of Gordon and Norris).

The experimental C^* performance curves peaked at O/F ratios that ranged from 0.8 to 2.0, the majority being around 1.5. The peak performance varied from 4200 to 5200 feet per second (1282 to 1585 m/sec), which is approximately 80 to 93 percent of the calculated theoretical.

Because two different propellant-injection methods were used, the C^* performance of thrustor 4 is shown with three different average curves in figure 7. For one series of tests, the fuel was injected into the combustion chamber through the port designed for the oxidizer, and the oxidizer was injected through the two ports designed for the fuel. The resulting data are represented by the solid curve between an O/F of 0.4 and 0.8. In the second series of tests, the method of fuel injection was reversed, and the resulting data are represented by the solid curve between an O/F of 0.8 and 1.4. For tests of the same time duration, the C^* performance was much lower for the second test series than for the first. When the second test series was continued for durations of 1200 percent longer than the first series, the performance tended to match in each case. The performance curves do not overlap from one injection technique to the other because the injection pressure limited the extent to which the O/F variations could be carried. A possible explanation for this variation in combustion performance is that, in the first test series, with two oxidizer jets impinging on one axial fuel jet, the combustor walls are covered with oxidizer spray and rapidly heat; this heating effect, in turn, improves the vaporization and reaction of the fuel with the oxidizer. With two fuel jets impinging on an axial oxidizer jet, the resulting fuel spray tends to keep the combustor walls cooled, and vaporization and propellant reaction are less efficient until the combustor walls reach the same operating temperature as in the first test series.

Thrustor 3 has the same type of propellant injection as do thrustors 2 and 6; however, its performance is 92 percent of theoretical as compared with 84 and 80 percent for the other two thrustors. The differences in the performance of thrustor 3 and thrustors 2 and 6 may be explained by their respective combustion-chamber length-to-diameter ratios; for thrustor 3, the ratio was 7.5 as compared with 3.2 for thrustor 2 and 2.3 for thrustor 6. The large ratio of thrustor 3 affects its performance because the propellant injection ports are much closer to the hot inner combustor-wall surface, and the fuel jets have a longer chamber length to travel than they do in thrustors 2 and 6.

Another thrustor that gave a relatively high performance was number 7. Its

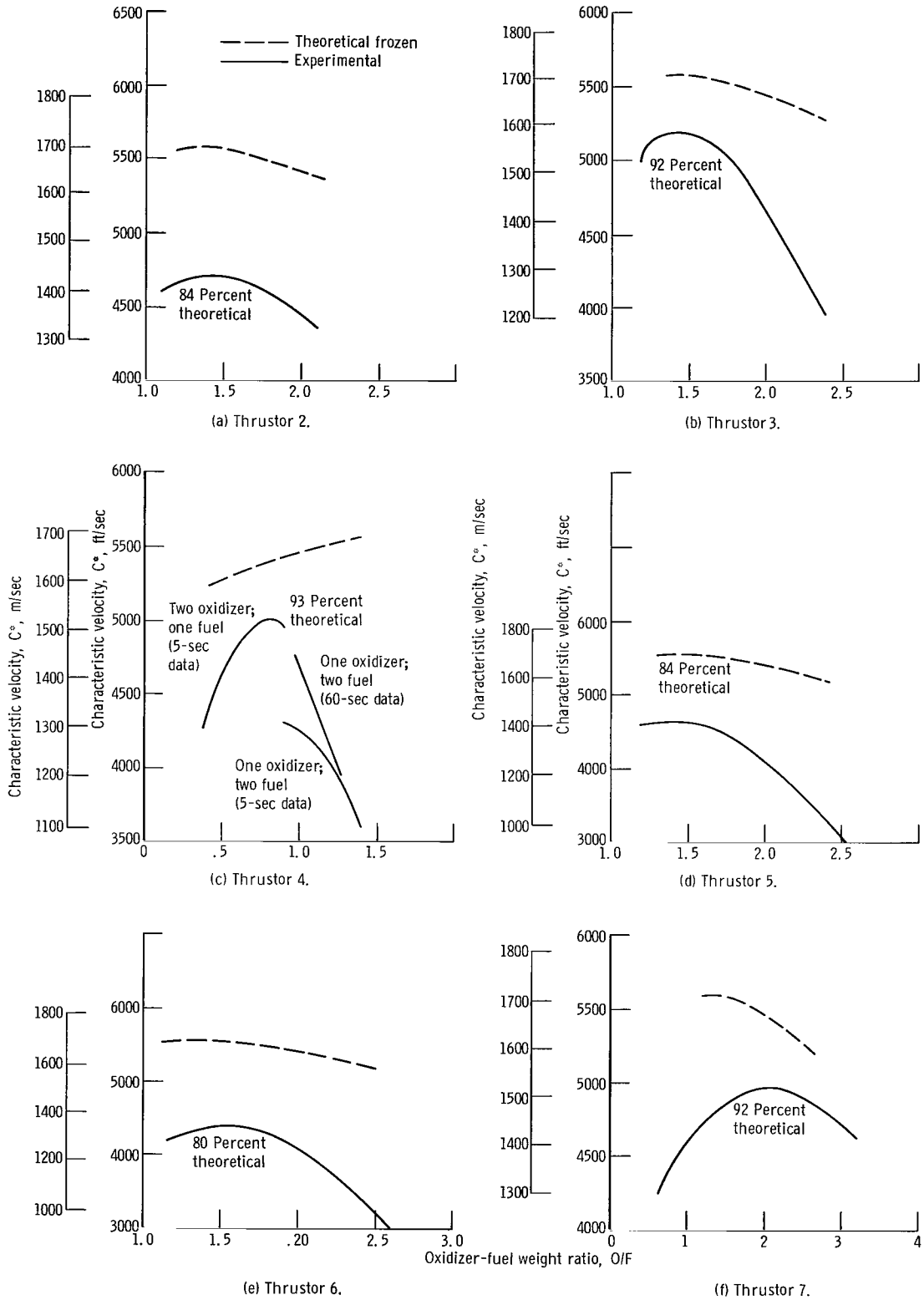

(a) Thrustor 2.

(b) Thrustor 3.

(c) Thrustor 4.

(d) Thrustor 5.

(e) Thrustor 6.

(f) Thrustor 7.

Figure 7. - Thrustor experimental characteristic velocity performance as function of propellant mixture ratio.

combustor-chamber length to diameter ratio is only 1.4, but it has a very large characteristic length L^* of 60 inches (152 cm) and uses a novel propellant injection technique. Propellant jet impingement is not depended on for jet breakup and vaporization; instead, the propellants are injected through atomization nozzles. Also, the resulting propellant mist is injected away from, rather than toward, the thrustor gas exit. These two steps improve the propellant reaction by permitting better utilization of the existing combustor volume; thus the combustion gas temperature is higher than that which would occur in a combustor having the same volume but using a more conventional injection technique.

The overall C^* performance of these thrustors is much lower than that of larger thrustors. For example, with 100-pound (444.8-N) thrust systems, C^* is expected to be higher than 5500 feet per second (1675 m/sec)(unpublished data obtained by Bell Aerosystems, Inc.). The combustion efficiency of the small thrustors is strongly influenced by the atomization, mixing, and reaction of the propellants within the combustor. With only two or three orifice jets to inject the propellants into the combustor, any slight misdirection or obstruction in a stream will drastically reduce the efficiency of the combustion process.

Specific impulse as function of oxidizer-fuel ratio. - The specific impulse of each thrustor firing in a vacuum environment was determined at steady-state operating conditions by dividing the thrust data by the total propellant flow rate obtained at the same time:

$$I_{sp} = \frac{F}{W_t}$$

During testing, the vacuum environment was maintained so that the thrustor nozzles were always flowing full or, possibly, were flowing underexpanded.

The specific impulse efficiency is defined as the ratio of the experimentally determined I_{sp} to the theoretical I_{sp}. The theoretical I_{sp} was determined on the basis of frozen composition conditions; that is, the combustion products flowing through the thrustor throat and nozzle did not change in composition. The experimental and theoretical I_{sp} for each of the thrustors is plotted as a function of O/F in figure 8, where the experimental data are presented as an average curve. With regard to performance and O/F, the deviation from this curve was ±4 percent.

The experimental I_{sp} performance curves of figure 8 are similar to the C^* curves of figure 7: the maximum I_{sp} was obtained at O/F ratios that ranged from 1.0 to 2.0, with most of the I_{sp} values reaching a peak at about 1.5. The peak values varied from 195 to 262 pounds thrust per pound of propellant flow per second (1912 to 2570 (N)(sec)/kg). These values are approximately 67 to 84 percent of the theoretical values obtained at a corresponding O/F ratio. The two performance curves in figure 8 for thrustor 4 are

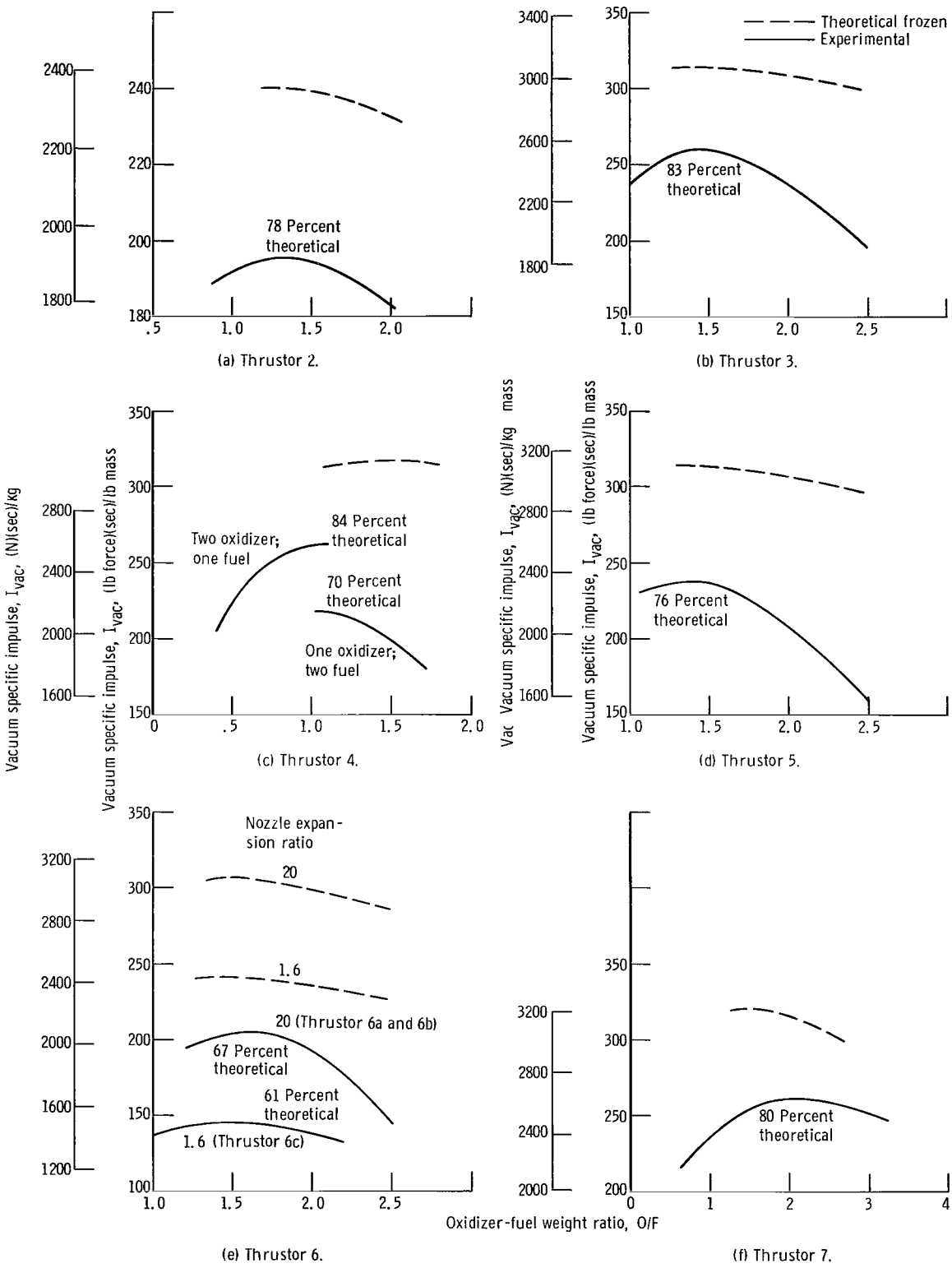

(a) Thrustor 2.

(b) Thrustor 3.

(c) Thrustor 4.

(d) Thrustor 5.

(e) Thrustor 6.

(f) Thrustor 7.

Figure 8. - Thrustor experimental vacuum specific impulse performance as function of propellant mixture ratio for tests of more than 500 milliseconds duration.

presented similarly to those in figure 7 for the characteristic performance. Two performance curves are also presented for thrustor 6 in figure 8, but in this case three nozzles were used; two of the nozzles (6a and 6b) had an expansion ratio greater than 20 and the other nozzle (6c) had an expansion ratio of 1.6 (sea-level expansion). All the nozzles were used on the thrustor tested in a vacuum environment. The larger expansion ratio did increase the specific impulse efficiency.

With rocket engines having a larger thrust (25 lb force or more or 110 N), the specific impulse efficiency is generally slightly less than the characteristic velocity efficiency (4 to 6 percentage points, unpublished data obtained by Marquardt Corp.). However, in the case of these small thrustors, the difference between the two performance parameters is 6 to 13 percentage points. The interrelation between the characteristic velocity and specific impulse performance is the thrust-coefficient: $C_f = I_{sp}\, g_c/C^*$. Using this equation with the available experimental data gives C_f data between 1.38 and 1.82. These values of C_f are 90 to 98 percent of theoretical (ref. 1). The C_f factor is also equal to the thrust divided by the thrustor throat area and the combustion-chamber pres-

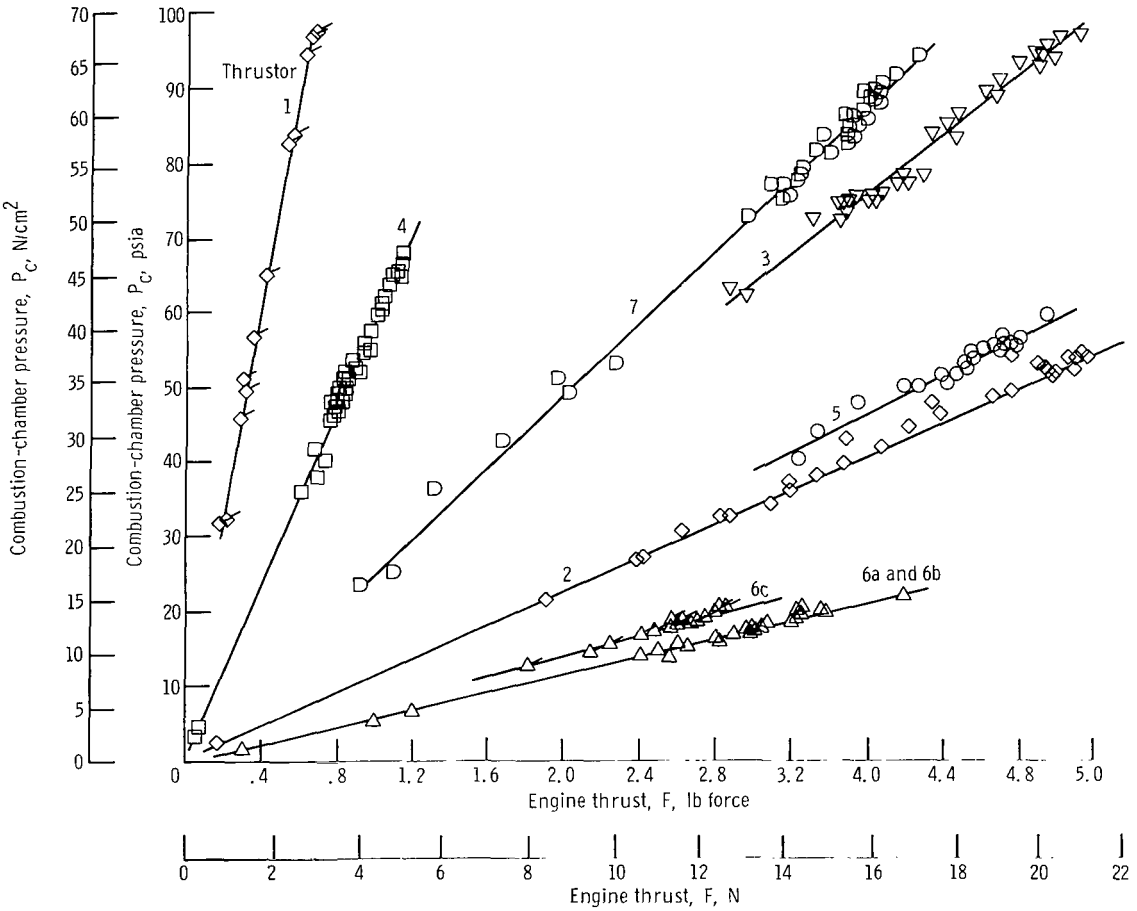

Figure 9. - Engine chamber pressure as function of thrust.

sure, $C_f = F/(A_t)(P_c)$. A plot of the experimental combustion-chamber pressure against the thrustor experimental thrust data (fig. 9) indicates that the thrust coefficient for each thrustor is very near to being a constant over the experimental testing range. Thus, with the thrust coefficient remaining relatively high (90 percent or more), a loss in overall performance I_{sp} for these small thrustors is due primarily to poor propellant combustion C^*.

Pulsing Performance

Total impulse. - The thrustor total impulse I_t is defined as the thrust integrated as a function of time, $\int_{t=0}^{t=n} F\,dt = I_t$. This integration was performed for each test by the thrust-stand electronic network. The I_t indicates the total force that will be obtained from a thrustor operating for a given time duration. By itself, I_t does not indicate how efficiently the thrustor is producing the thrust.

Each thrustor was tested over a range of operational time durations. Enough tests were made at any one time duration to establish repeatable impulse data. The impulse data as a function of test time are shown for each thrustor in figure 10. The data from all the thrustors show a direct, almost linear, relation between the experimental impulse and the valve open-time. As the pulse on-time becomes a greater percentage of the total operating time, the nearer the performance comes to theoretical impulse. This relation is illustrated in figure 10 with data for thrustors 6 and 7. The individual test durations were held constant while the time between pulses was increased.

Specific impulse as function of operating time. - As mentioned in the section, APPARATUS AND PROCEDURE, for tests of less than 500 milliseconds, little credibility is placed in the data at a given instant during the test, and integrated and average data values are used to calculate the performance. In this section, the I_{sp} is determined as a function of decreasing operating time (less than 500 m sec) with the O/F held relatively constant from test to test. Tests were repeated at identical conditions often enough to get identical, repeatable data. Thus, the I_{sp} in this section is an average value over the time span of the test.

The average I_{sp} data for each of the thrustors over a range of valve on-times is shown as an average curve in figure 11. While it was possible to obtain impulse data (fig. 10) down to 10 milliseconds, the slow response time of the propellant flowmeters placed a lower limit of about 20 milliseconds on the flow data. Therefore, 20 milliseconds is also the lower limit on the I_{sp} data shown in figure 11. The I_{sp} performance decreases rapidly for all the thrustors from the peak values (as shown in fig. 8) to less than 25 percent of the peak value in some cases at the minimum valve on-time.

Two performance curves, each representing different propellant injection techniques

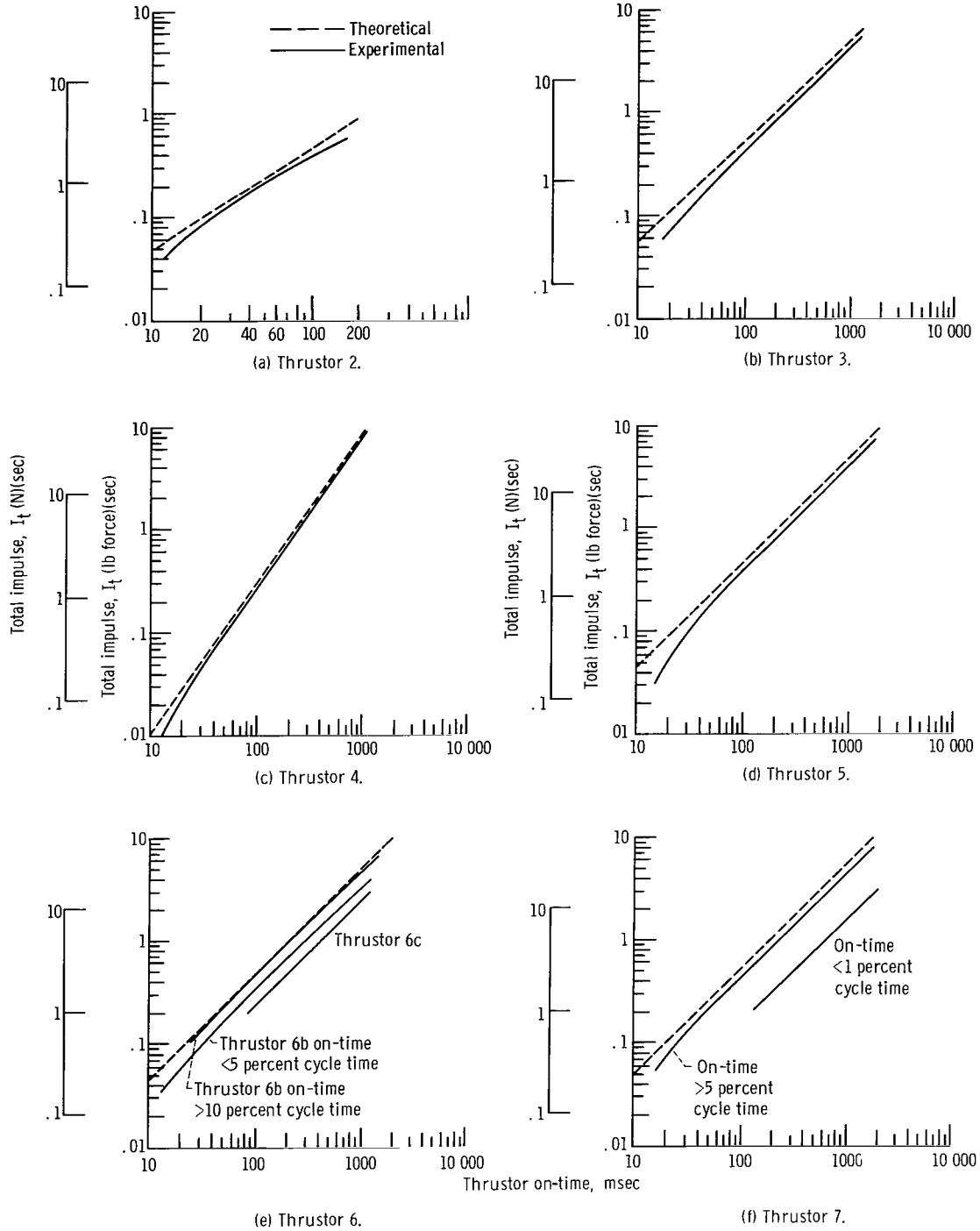

(a) Thrustor 2.

(b) Thrustor 3.

(c) Thrustor 4.

(d) Thrustor 5.

(e) Thrustor 6.

(f) Thrustor 7.

Figure 10. - Thrustor experimental total impulse as function of thrustor on-time.

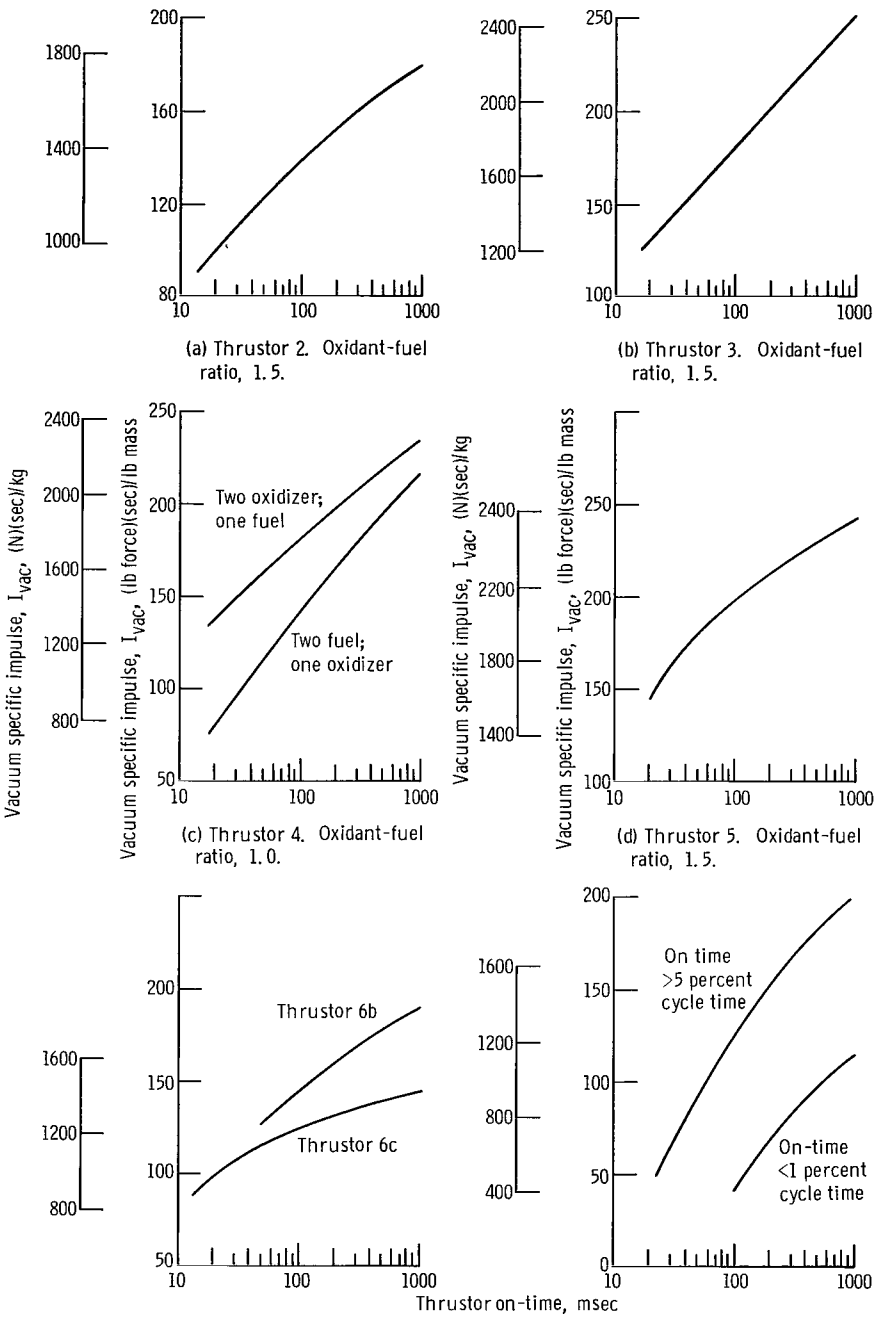

(a) Thrustor 2. Oxidant-fuel ratio, 1.5.

(b) Thrustor 3. Oxidant-fuel ratio, 1.5.

(c) Thrustor 4. Oxidant-fuel ratio, 1.0.

(d) Thrustor 5. Oxidant-fuel ratio, 1.5.

(e) Thrustor 6. Oxidant-fuel ratio, 1.5.

(f) Thrustor 7.

Figure 11. - Thrustor experimental vacuum specific impulse performance drop-off as function of thrustor on-time.

used, are shown in figure 11(c) for thrustor 4. For thrustor 6 (fig. 11(e)) two performance curves, each for a different nozzle-expansion ratio, appear to be converging at some minimum valve on-time.

The fact that decreasing valve off-time between tests or pulses resulted in higher I_t is also shown with I_{sp}. For example, in figure 11(f) performance curves are presented for thrustor 7 operating with a duty cycle of more than 5 percent and less than 1 percent. The curves show that, for a given on-time and a constant O/F, performance increases as the on time becomes a larger percentage of the total test time.

Since most of the I_t performance is very close to theoretical values (fig. 10) and the I_{sp} for the same thrustors falls off rapidly with decreased operation time, the propellant utilization is apparently very poor. When the propellant control valves open, the propellant must surge into the vacuum environment of the combustion chamber. This surging is shown by spikes in the data traces (especially for the oxidizer) of figures 5 and 6. For short tests, neither flows nor thrust has time to reach equilibrium conditions, and repeated tests become a series of detonations. The actual O/F during this surging

TABLE III. - THRUSTOR AVERAGE RESPONSE TIMES FOR TORQUE- AND SOLENOID-TYPE VALVES

[Data are average values for thrustor test times of 1 sec or longer.]

Thrustor	Average time, m sec, from start until-					Average time, m sec, from stop signal until-				
	Propellant flow begins	Chamber pressure begins to increase	Thrust begins to increase	Chamber pressure is approximately 90 percent of maximum	Thrust reaches maximum test value	Propellant flow stops	Chamber pressure begins to decrease	Thrust begins to decrease	Chamber pressure is approximately 10 percent of maximum	Thrust reaches prerun value
1	10	17	23	134	---	---	---	---	---	---
2	11	17	25	177	35	7	8	7	245	23
3	14	19	18	210	30	7	7	8	280	21
4	10	51	53	177	109	6	6	10	64	30
5	4	29	31	60	50	3	5	9	119	316
6	10	14	16	323	26	7	5	8	122	27
[a]7	6	276	305	644	704	3	5	9	119	316
[b]7	6	---	---	---	---	5	---	15	---	342

[a]With value 8.

[b]With value 9.

of propellants is apparently much different from what it would be once flows and thrust have stabilized. For the very short pulse durations, the propellant valve opens and starts to close before the thrust and flows reach their maximum values (see fig. 6). It is little wonder, then, that combustion efficiency is so low for the short valve on-times. The thrust (and I_t) produced is a result of high initial flow rates, propellant vaporizing, and burning to some degree, and then expanding out through the thrustor nozzle. For these short tests, no matter how often they are repeated, the combustor wall temperature increases little.

Thrustor propellant valve response time. - A limitation of how often or how fast a thrustor can be fired is the opening and closing response time to an electrical signal. In this investigation, the valve response time is defined as the time from the initiation or termination of the valve power to the time that a change in propellant flow downstream of the valve is indicated. From data such as that shown in figure 6, an average response time was computed for each of the valves tested. These data are presented in table III in the columns "Propellant flow begins", and "Propellant flow stops". These response time averages ranged from 4 to 14 milliseconds in opening and 3 to 7 milliseconds in closing. The averages were distributed between the torque- and solenoid-type valves so that neither had an apparent response superiority over the other.

Thrustor ignition response time. - Another limitation on the pulse or repeated firing of a small thrustor is the time necessary for the propellants to react and to produce pressure and thrust. This time is called ignition delay and is the period that begins when the propellant is detected in the thrustor injector and ends when a sudden change is noted in the thrust signal. Again, the average ignition delay was determined for each of the thrustors, and these values are presented in table II. In figure 12, these data are presented as a function of the thrustor characteristic length L^*, which is defined as the combustor volume divided by the cross-sectional area of the combustor nozzle throat. As the L^* increases, a longer time is required for the propellants to vaporize and mix and to reach an ignition temperature condition. The ignition delay data of figure 12 are for tests in which the combustor and propellants are both at ambient temperatures. For repeated firings with the same thrustor, the combustor-wall temperature increased with each firing, and the ignition delay decreased accordingly. The shorter the off-times between pulses, the shorter the ignition delay time. This relation between off-time and ignition delay is shown in figure 13 for thrustors 3 and 7. The ignition delay for the initial firings of either thrustor is that shown in figure 12. As firings were continued, this delay decreased until it reached a constant value dependent on the off-time between firings or pulses. As the off-time was decreased, both thrustors reached an almost identical ignition delay that approached zero at zero off-time (steady-state firing conditions).

Thrustor performance response time. - The final limitation to obtaining a particular impulse or thrust is the time required to reach the desired impulse or thrust value from

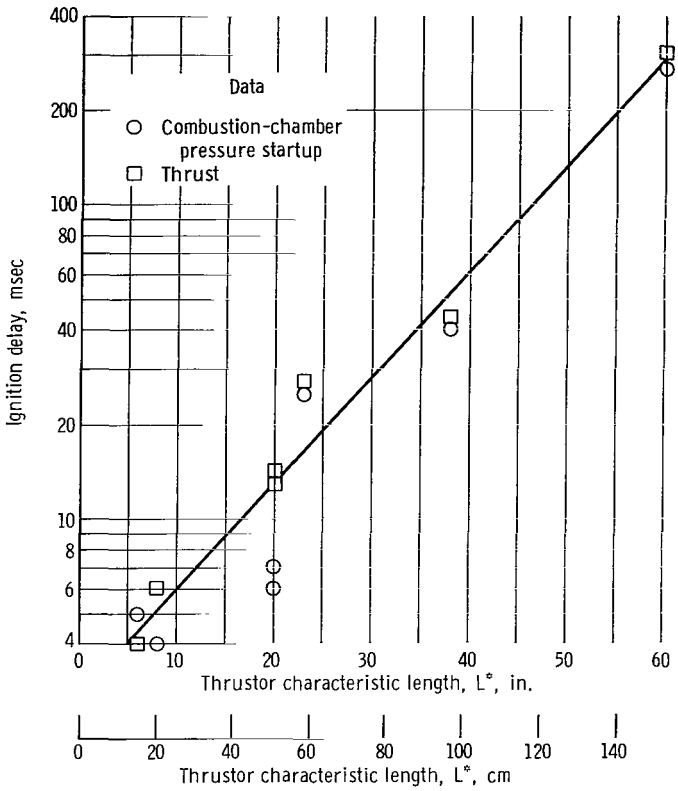

Figure 12. - Thrustor ignition delay as function of thrustor characteristic length.

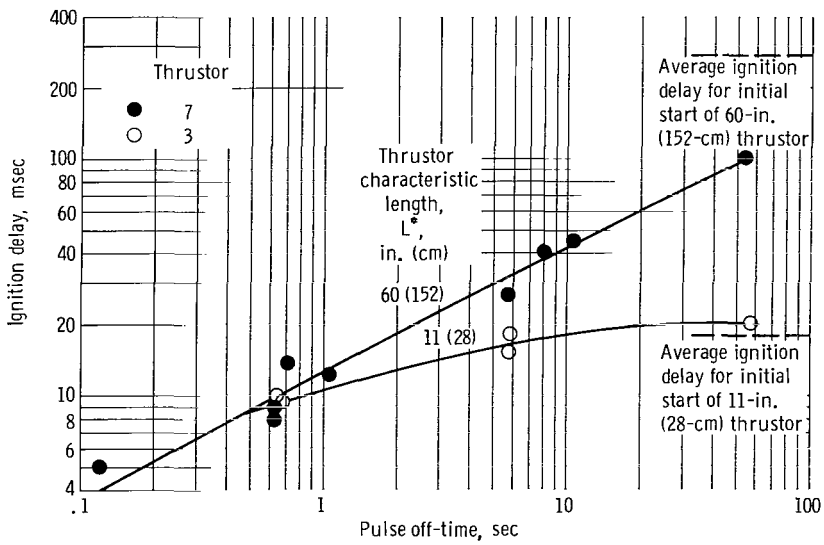

Figure 13. - Average ignition delay after start of pulsing operation. (Delay, time from start signal until chamber pressure starts to rise.)

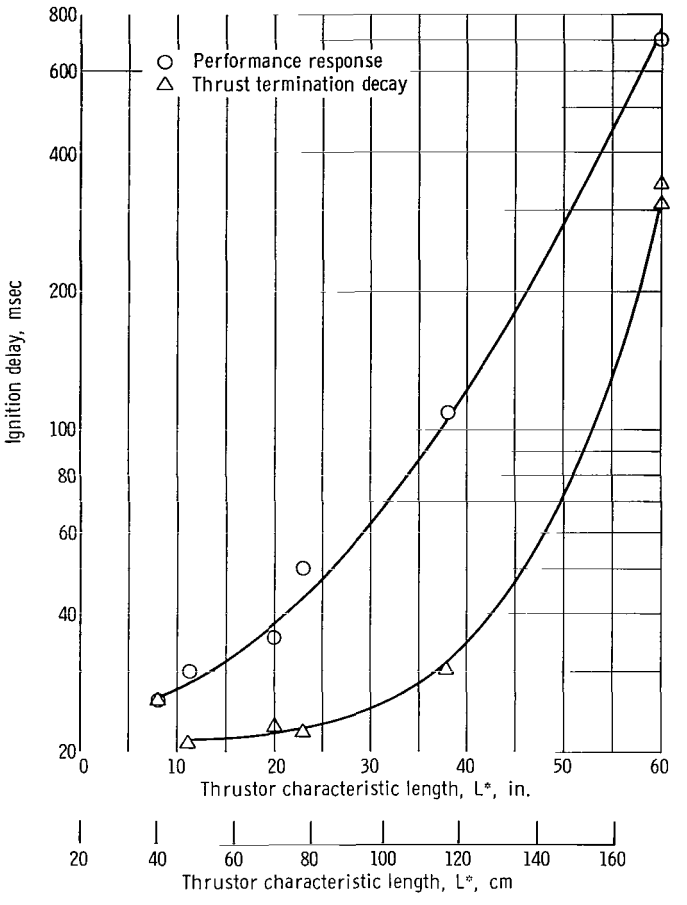

Figure 14. - Thrust buildup and fall-off delay.

the time an actuation signal is given. This performance response time was calculated and averaged for each of the thrustors and is presented in table II. The performance response time includes both the valve response and ignition delay times plus the time for the thrust to build up to its maximum equilibrium value. Therefore, the thrust or performance response is also a function of the L^*, as shown in figure 14.

Also important in the performance response of a thrustor is thrust decay on signal termination. Because thrust decay does not involve an ignition delay, it is a much shorter time than the startup response. The curve for this termination decay is also shown in figure 14. Both the curves in figure 14 are for initial firings, that is, when the combustor and propellants are at ambient temperatures. As the thrustor temperature increases with successive operations, the ignition time decreases, which results in a shorter performance response time.

In computing the performance response, maximum and minimum values of thrust were used rather than the combustion-chamber pressure maximum and minimum re-

sponse times. The large difference in maximum and minimum response times between the thrust and the chamber pressure is shown in table III. Although chamber pressure and thrust data have a linear correlation for a given thrustor, as shown in figure 9, each signal arrives at this correlation at a different rate. The chamber-pressure change rate is felt to be restricted by combustion-gas sonic flow-rate limits in the measuring transducer (this limitation is discussed in the appendix). The thrust data are believed to reflect more accurately the actual thrustor response behavior.

Thrustor Heat Transfer

Another criterion to be considered in the design and operation of small thrustors is the material temperature limits. The theoretical combustion temperature of nitrogen tetroxide and a mixture of 50 percent UDMH and 50 percent hydrazine is 5500° to 6000° F (3300° to 3600° K) for the testing conditions of the present investigation. The amount of heat reaching the combustor walls is a function of the amount of the propellant that merely cools the walls rather than that which enters into the combustion process. As mentioned in the section, APPARATUS AND PROCEDURE, all the thrustors had either radiation-cooled walls or heat-sink walls.

The importance of temperature was observed during the tests. If the individual pulse-run firings were kept short enough or the time between firings increased enough, all the thrustors tested could pulse fire for long periods of time without an excessive heat buildup in the combustor walls. However, as the individual firings increased in duration and/or the down time (or off-time) was decreased, the combustor-wall temperature increased rapidly. In table IV, the temperature data for thrustor 3 illustrate this phenomenon. Table IV(a) presents 10 successive 1/2-second firings with the wall temperatures at the end of each firing, and IV(b) presents the data for a continuous firing that was terminated when the combustor wall burned through. Thrustor 3 had a relatively high C^* performance level, which indicated that most of the propellant was going into the combustion reaction. This temperature rise as a function of run time is plotted in figure 15, along with data for thrustor 3 and the wall temperature data for several other thrustors. An example of a continuous operational radiation-cooled thrustor is thrustor 4, which reached an equilibrium wall temperature of about 1900° F (1300° K) after about 60 seconds of steady operating conditions. Thrustors with lower performance tended to reach a lower wall temperature equilibrium.

TABLE IV. - THRUSTOR 3 PULSING AND STEADY-STATE TESTS

(a) Pulsing test; on time, 0.470 second; off time, 5.90 seconds

Pulse	Maximum combustion pressure		Maximum thrust		Impulse		Combustor wall temperature			
							Throat		Chamber	
	N/cm^2	psia	N	lb force	N-sec	lb force-sec	^oK	^oF	^oK	^oF
1	60.5	88	18.9	4.25	----	---	494	428	484	410
2	60.5	88	18.9	4.25	----	---	567	557	558	544
3	61.3	89	----	----	8.90	2.0	619	651	625	664
4	61.3	89	----	----	8.45	1.9	669	739	681	765
5	60.5	88	----	----	8.90	2.0	721	835	723	840
6	59.8	87	----	----	↓	↓	765	912	764	912
7	59.8	87	----	----	↓	↓	798	976	793	967
8	60.5	88	----	----	↓	↓	828	1026	821	1018
9	59.8	87	----	----	8.45	1.9	847	1061	846	1061
10	59.8	87	18.8	4.22	----	---	900	1158	858	1082

(b) Steady-state test; total run time, 10 seconds

Time after start of run, sec	Combustion-chamber pressure		Thrust		Oxidant-fuel ratio	Combustor wall temperature			
						Throat		Chamber	
	N/cm^2	psia	N	lb force		^oK	^oF	^oK	^oF
0	34.4	0.05	0	0	---	413	284	406	271
1	61.3	89	19.6	4.41	1.4	508	454	503	445
2	61.3	89	19.5	4.38	1.5	592	604	636	686
3	60.5	88	19.4	4.37	↓	696	791	877	1120
4	↓	↓	↓	4.35	↓	767	920	1175	1653
5	↓	↓	↓	4.35	↓	850	1069	1330	1933
6	↓	↓	↓	4.35	↓	980	1306	1468	2179
7	59.8	87	19.3	4.33	↓	1082	1489	1500	2240
8	59.8	87	19.2	4.31	↓	1207	1710	1570	2371

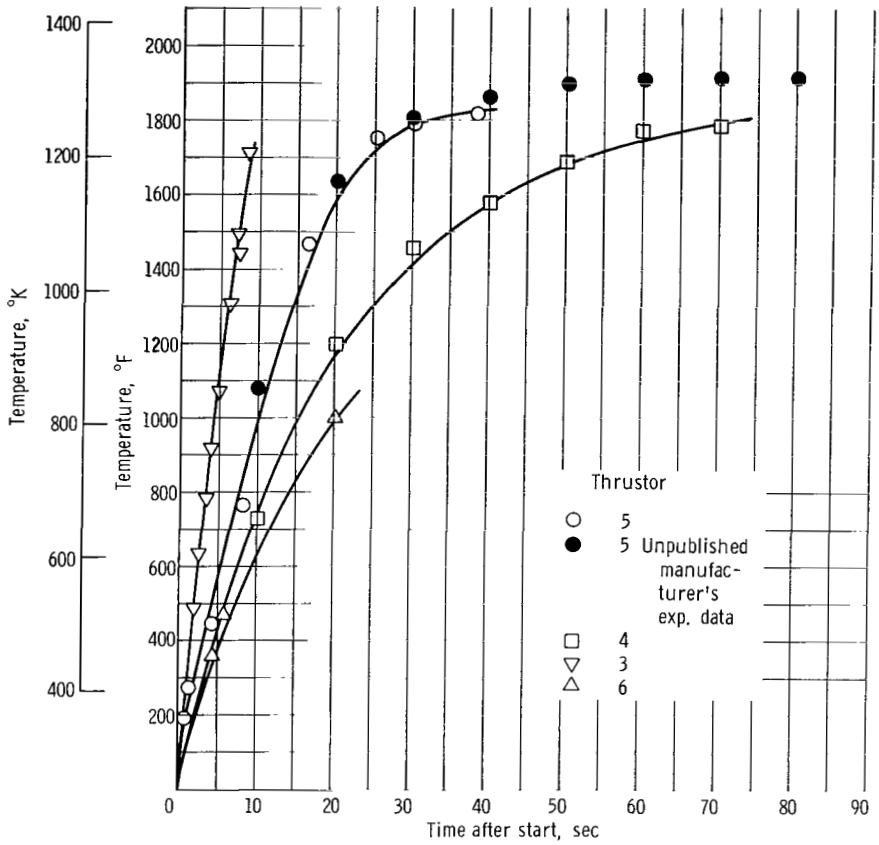

Figure 15. - Throat wall temperature as function of run duration.

SUMMARY OF RESULTS

As a result of this investigation of reaction control, storable bipropellant thrustors, the following conclusions were established:

1. The steady-state performance for firing times longer than 500 milliseconds is about 80 to 90 percent of theoretical in terms of characteristic velocity, and 67 to 84 percent of theoretical in terms of specific impulse. The thrust coefficient remained relatively high (90 percent or more of theoretical). The low specific impulse results are due primarily to poor propellant combustion efficiency, that is, low characteristic exhaust velocity.

2. The pulse-firing data indicated a direct, almost linear, relation between the experimental total impulse and the valve open-time down to approximately 10 milliseconds. For the same pulses, however, the average specific impulse decreased to approximately one-fourth of the steady-state performance value.

Lewis Research Center,
National Aeronautics and Space Administration,
Cleveland, Ohio, September 11, 1967,
128-31-20-50-22.

APPENDIX - TEST EQUIPMENT DETAILS

Multipound Thrust Stand

The thrust stand assembly consists of a mass-balanced platform system, pivoted on knife edges and restrained by an electric-force motor that is controlled by a displacement pickup and electronic network. The system is designed to measure thrust from 0.01 to 10 pounds force (0.044 to 44.5 N) in four range settings with a threshold of 1 percent of any range setting. Impulse can be measured from 0.01 to 10 pound-seconds (0.044 to 44.5 N-sec) with the same accuracy as that for thrust. Thrust variations can also be measured with the same accuracy at frequencies up to 100 cps (100 Hz).

The mass-balanced platform system is suspended on six sets of precision knife edges and bearing blocks. The platform counterbalances are remotely adjustable by electric motors, and they permit the platform to be balanced for a payload of up to 25 pounds (11.3 kg). The moving elements of the displacement transducer and of the force motor are connected directly to the platform. Propellants and other service fluids are brought to the thrustor platform through flexible tubing parallel to the pivots. The electrical wiring is set up in a similar manner. The electronic equipment associated with the force-generating loop and balancing is remotely located.

The combination of accurate force readout and high frequency response is obtained by a force-generating servosystem that operates in the following manner: The force from the thrustor under study causes a horizontal platform displacement and results in a voltage output from the displacement transducer. This signal, after suitable amplification and compensation for loop phase shift, is applied to the force motor that produces a force opposing that from the thrustor and displaces the platform toward null position. At null position, the force exerted by the force motor is in balance with the force produced by the thrustor. The current in the force motor is proportional to the force produced and is used as the thrust readout for the system. This system is described in detail in reference 2.

Propellant Flowmeters

A major problem in testing millipound thrustors is determining the propellant flow rates. An average flow rate can be obtained by determining the total amount of propellant used for a fixed duration of time; however, in this investigation, measurement of the instantaneous flow rates for each propellant was attempted. The flow rates for the mixture of 50 percent UDMH and 50 percent hydrazine ranged from 0.0008 to 0.0049 pound per second (0.364 to 2.04 g/sec) and for nitrogen tetroxide from 0.0020 to 0.0100

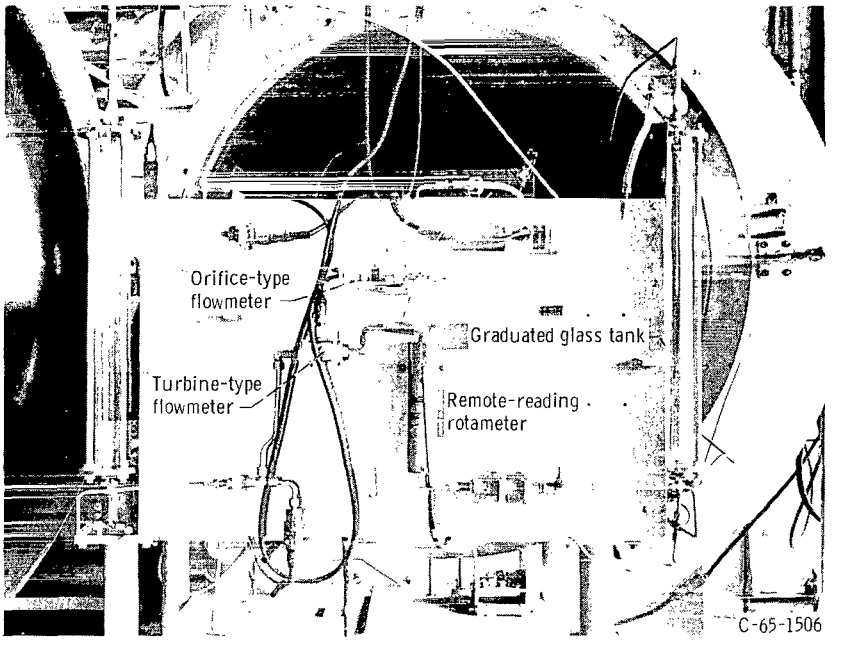

Figure 16. - Flowmeter calibrator.

pound per second (0.91 to 4.54 g/sec). Three different types of flowmeters were selected that could operate with these propellants and indicate the flow rates. These flowmeters, a differential pressure orifice, a turbine wheel, and a remote-reading rotameter, are shown in figure 16. The meters were calibrated (in the rig pictured in fig. 16) by flowing actual propellants from one glass tank to another through the meters. The indicated flow rates from each of the flowmeters were thus checked against each other and against the visual amount of propellant that had flowed from one glass tank to the other within a given time interval. Different pressure heads in the propellant tanks were used to obtain different flow rates. The calibrated flow rates had an accuracy of at least 0.0002 pound per second (0.091 g/sec).

Thrustor Combustion-Chamber Pressure Measurements

The combustion chamber pressure was measured on most of the thrustors by a pressure transducer connected by a finite length of metal tubing to the combustion chamber or to the propellant injector face. Most of the thrustors were so small physically that this connecting tube was capillary size with a large length-diameter ratio.

Although the pressure transducers have a high natural frequency capability (2 to 6 kHz), when they are connected to the pressure source with a high length-diameter tube, their frequency response is drastically reduced. The pressure measuring system then

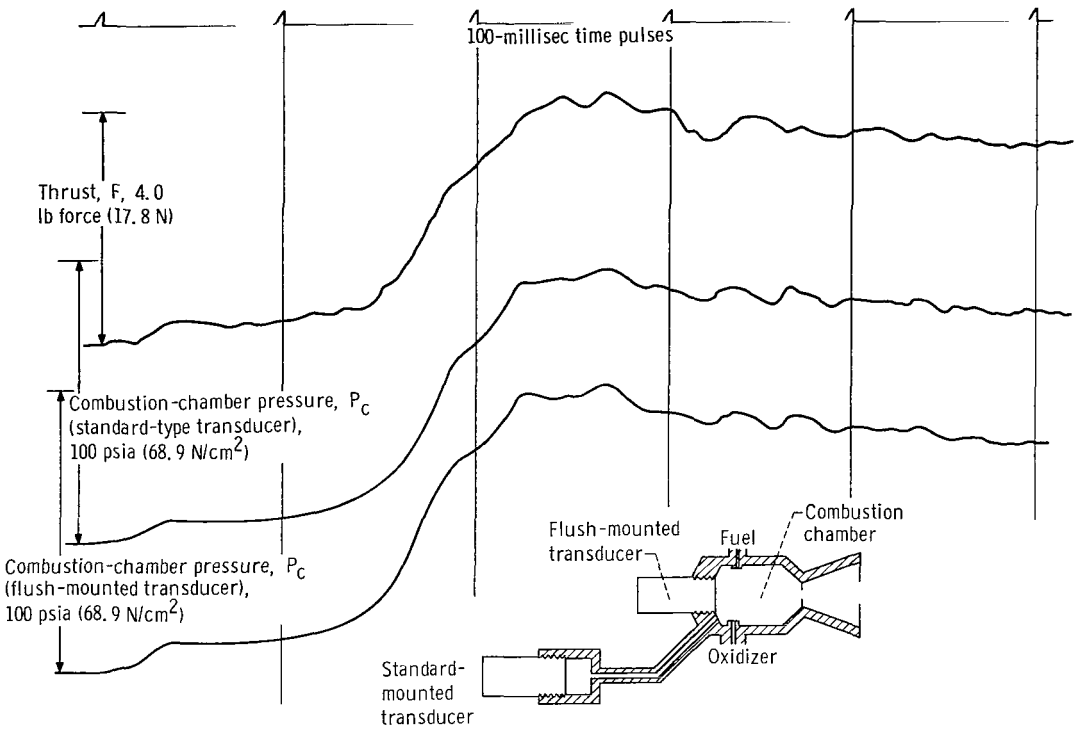

Figure 17. - Comparison of initial thrust, flush transducer chamber pressure, and standard-type transducer chamber pressure.

resembles a Helmholtz resonator. Resonator equations indicate a typical frequency response of about 166 hertz for a setup such as that used in this investigation.

In order to obtain experimental verification of this frequency response, dual chamber-pressure measuring transducers were installed on several thrustors. On thrustor 7, one pressure transducer was connected by the metal tubing, and a flush-mounted transducer was mounted directly in the combustor wall (see sketch in fig. 17). Because the flush-mounted transducer was uncooled, its data were only accurate for a few seconds of any given test. A typical oscillograph record of the two transducers and of the thrust system is presented in figure 17. The agreement between the two pressure measuring systems for time spans of a few milliseconds appears very good, with some evidence of agreement for time spans as short as a millisecond, thus providing reasonable verificiation of the calculated frequency response.

Thrustor Wall Temperature Measurements

Temperature measurement of the thrustor combustor walls, especially those made of refractory materials, proved to be a problem. Mounting thermocouples solidly to the refractory metal combustor walls involved breaking through the protective coating on the

material, thereby risking oxidation failure at that point during high-temperature conditions. Optical means of determining accurate wall temperatures were complicated because the thrustors were operated in a vacuum tank that was filled with haze and fumes during actual tests and because emissivity data for coated refractory materials at high temperatures were lacking.

One solution to the problems in making temperature measurements was to wire thermocouples to the refractory material thrustor walls. First the wired-on thermocouple was calibrated in the following manner. Two identical thermocouples were mounted as close together as possible on a stainless-steel chamber. One thermocouple was welded to the stainless surface, and the other thermocouple was wired onto the chamber. During testing with the stainless-steel chamber, a ratio was established between the temperature data from the two thermocouples. Then the wired-on thermocouple was remounted on the refractory metal chamber. The data obtained by the wired-on thermocouple during testing were then multiplied by the ratio determined from the tests with the stainless-steel chamber. This corrected temperature is the one reported in this investigation for refractory material thrustors. The actual temperatures are reported only for those thrustors having stainless-steel combustors.

REFERENCES

1. Sutton, George P.: Rocket Propulsion Elements. Second ed., John Wiley and Sons, Inc., 1956, p. 70.

2. Smith, J. D.: Modification to Government-Owned Thrust Stand System. Hughes Research Labs. (NASA CR-72021), Aug. 1966.

NASA-Langley, 1968 — 28 E-3671

"The aeronautical and space activities of the United States shall be conducted so as to contribute . . . to the expansion of human knowledge of phenomena in the atmosphere and space. The Administration shall provide for the widest practicable and appropriate dissemination of information concerning its activities and the results thereof."

—NATIONAL AERONAUTICS AND SPACE ACT OF 1958

NASA SCIENTIFIC AND TECHNICAL PUBLICATIONS

TECHNICAL REPORTS: Scientific and technical information considered important, complete, and a lasting contribution to existing knowledge.

TECHNICAL NOTES: Information less broad in scope but nevertheless of importance as a contribution to existing knowledge.

TECHNICAL MEMORANDUMS: Information receiving limited distribution because of preliminary data, security classification, or other reasons.

CONTRACTOR REPORTS: Scientific and technical information generated under a NASA contract or grant and considered an important contribution to existing knowledge.

TECHNICAL TRANSLATIONS: Information published in a foreign language considered to merit NASA distribution in English.

SPECIAL PUBLICATIONS: Information derived from or of value to NASA activities. Publications include conference proceedings, monographs, data compilations, handbooks, sourcebooks, and special bibliographies.

TECHNOLOGY UTILIZATION PUBLICATIONS: Information on technology used by NASA that may be of particular interest in commercial and other non-aerospace applications. Publications include Tech Briefs, Technology Utilization Reports and Notes, and Technology Surveys.

Details on the availability of these publications may be obtained from:

SCIENTIFIC AND TECHNICAL INFORMATION DIVISION

NATIONAL AERONAUTICS AND SPACE ADMINISTRATION

Washington, D.C. 20546